

Enhancement of Laccase Activity through the Construction and Breakdown of a Hydrogen Bond at the Type I Copper Center in *Escherichia coli* CueO and the Deletion Mutant $\Delta\alpha 5-7$ CueO[†]

Kunishige Kataoka,[‡] Shun Hirota,[§] Yasuo Maeda,[‡] Hiroki Kogi,[‡] Naoya Shinohara,[‡]
Madoka Sekimoto,[‡] and Takeshi Sakurai^{*‡}

[‡]Graduate School of Natural Science and Technology, Kanazawa University, Kanazawa 920-1192, Japan, and [§]Graduate School of Materials Science, Nara Institute of Science and Technology, Ikoma, Nara 630-0192, Japan

Received July 11, 2010; Revised Manuscript Received December 8, 2010

ABSTRACT: CueO is a multicopper oxidase involved in a copper efflux system of *Escherichia coli* and has high cuprous oxidase activity but little or no oxidizing activity toward various organic substances. However, its activity toward oxidization of organic substrates was found to be considerably increased by the removal of the methionine-rich helical segment that covers the substrate-binding site ($\Delta\alpha 5-7$ CueO) [Kataoka, K., et al. (2007) *J. Mol. Biol.* 373, 141]. In the study presented here, mutations at Pro444 to construct a second NH–S hydrogen bond between the backbone amide and coordinating Cys500 thiolate of the type I copper are shown to result in positive shifts in the redox potential of this copper center and enhanced oxidase activity in CueO. Analogous enhancement of the activity of $\Delta\alpha 5-7$ CueO has been identified only in the Pro444Gly mutant because Pro444 mutants limit the incorporation of copper ions into the trinuclear copper center. The activities of both CueO and $\Delta\alpha 5-7$ CueO were also enhanced by mutations to break down the hydrogen bond between the imidazole group of His443 that is coordinated to the type I copper and the β -carboxy group of Asp439 that is located in the outer sphere of the type I copper center. A synergetic effect of the positive shift in the redox potential of the type I copper center and the increase in enzyme activity has been achieved by the double mutation of Pro444 and Asp439 of CueO. Absorption, circular dichroism, and resonance Raman spectra indicate that the characteristics of the Cu(II)–S(Cys) bond were only minimally perturbed by mutations involving formation or disruption of a hydrogen bond from the coordinating groups to the type I copper. This study provides widely applicable strategies for tuning the activities of multicopper oxidases.

Escherichia coli CueO (copper efflux oxidase) is a multicopper oxidase (MCO)¹ with high cuprous oxidase activity but little or no oxidizing activity toward organic substrates because of its unique molecular architecture, which includes a methionine-rich segment in helices 5–7 that serves to cover the binding site of the cuprous ion substrate (1–5). Nevertheless, CueO has the same catalytic copper centers as other MCOs: the type I (T1) copper collects electrons from substrates, and the trinuclear copper center (TNC) that is comprised of a type II (T2) copper and a pair of type III (T3) coppers functions in the binding and reduction of dioxygen with the assistance of the adjacent acidic amino acids Asp112 and Glu506 (6–8). T1 copper is responsible for the charge transfer bands, His(N) \rightarrow Cu²⁺ at \sim 440 nm, Cys(S[−])_σ \rightarrow Cu²⁺ at \sim 520 nm, and Cys(S[−])_π \rightarrow Cu²⁺ at 610 nm,

as well as the d–d transition bands above 700 nm in the absorbance spectrum (9, 10). The T3 coppers are bridged with a hydroxide ion, and the complex has an intense charge transfer band arising from the OH[−] \rightarrow Cu²⁺ transition at \sim 330 nm. T2 copper does not have a conspicuous band in the visible region. T1 copper and T2 copper afford characteristic electron paramagnetic resonance (EPR) signals in contrast to the EPR-silent T3 coppers because of a strong antiferromagnetic interaction due to the bridged hydroxide. To study the function and reaction mechanism of CueO and apply it to biofuel cells, we have performed mutations and protein engineering of CueO (11, 12). By deleting the methionine-rich helical region from CueO (Pro367–His416), we significantly increased the oxidase activities of the resulting deletion mutant, $\Delta\alpha 5-7$ CueO, for organic substrates. When we made the Ser mutant of Cys500, which acts as a ligand to T1 copper, the T1 copper center became vacant, and a reaction intermediate could be trapped. This helped to reveal the mechanism of four-electron reduction of O₂ by MCOs (7). On the other hand, replacement of Met510 (which axially coordinates to T1 copper) with Gln, Ala, or Thr produced coordination of an oxygen atom from their side chains or from a water molecule, and substitution of Met510 with Phe, Leu, and Ile produced a vacant axial site (13). The redox potential of T1 copper was found to shift toward positive or negative potential with these mutations and was accompanied by an increase or decrease in the overall catalytic activities of CueO.

[†]This work was in part supported by a Grant-in-Aid for Scientific Research (21655061) from the Ministry of Education, Science, Sports and Culture of Japan (to T.S.) and by a grant from Mandom Corp.

^{*}To whom correspondence should be addressed: Division of Material Sciences, Graduate School of Natural Science and Technology, Kanazawa University, Kakuma, Kanazawa 920-1192, Japan. Phone: +81-76-264-5685. Fax: +81-76-264-5742. E-mail: ts0513@kenroku.kanazawa-u.ac.jp.

Abbreviations: MCO, multicopper oxidase; T1, type I; T2, type II; T3, type III; TNC, trinuclear copper center; EPR, electron paramagnetic resonance; $\Delta\alpha 5-7$ CueO, deletion mutant of CueO; rCueO, recombinant CueO; BCA, bicinchoninic acid; ABTS, 2,2′-azino-bis(3-ethylbenzothiazoline-6-sulfonic acid); CD, circular dichroism; SLAC, small laccase from *Streptomyces coelicolor*.

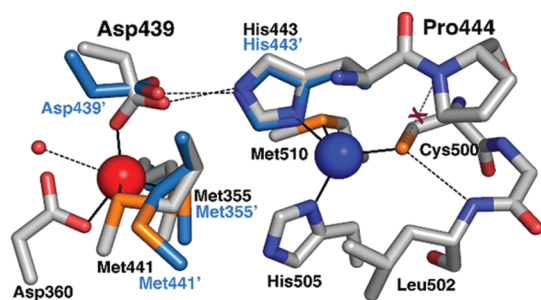


FIGURE 1: Structure of the T1 copper center in rCueO and $\Delta\alpha 5-7$ CueO (blue). T1 copper (blue) and substrate Cu^+ (red) are represented as spheres. Hydrogen bonds are shown as dashed lines. The figure was drawn with PyMOL (33) using coordinates from Protein Data Bank entries 1KV7 (rCueO) and 2YXV ($\Delta\alpha 5-7$ CueO).

The mutations described above were directed toward the coordinating amino acids (the inner-sphere group of T1 copper), while we previously showed that Asp112 and Glu506, which are located adjacent to the TNC and are directly and indirectly hydrogen-bonded with the ligand groups, also govern the activities of CueO via the binding of O_2 and donation of protons (6–8).

In this study, we mutated amino acids located near the T1 copper center to either form or disrupt a hydrogen bond involving a group coordinating to T1 copper of CueO. According to the crystal structures of a recombinant CueO (rCueO) and $\Delta\alpha 5-7$ CueO (11) (Figure 1), Asp439 is involved with the binding of cuprous ion and forms a hydrogen bond with His443 that is coordinated to T1 copper (3). Ceruloplasmin, a ferroxidase from vertebrates, has an analogous hydrogen bond between Glu272 (which is involved in the binding of Fe^{2+}) and His1026 (which is coordinated to T1 copper) (14). This hydrogen bond has been considered to provide an electron transfer pathway to connect the substrate-binding site to T1 copper. In a preliminary electrochemical study of the Asp439Ala mutant of rCueO, the redox potential of T1 copper was found to shift in the positive direction (15). This prompted us to characterize the Asp439Ala mutant in more detail by studying its enzymatic activities. With the shift in the redox potential, the driving force of the electron transfer between the substrate and T1 copper increased, although the putative electron transfer pathway between them was broken and the driving force of the subsequent intramolecular electron transfer between T1 copper and TNC was found to be decreased. In this study, our objective is to reveal the change in the thermodynamic driving force of electron transfer that dominates the overall activities of CueO.

Figure 1 shows that the thiolate group of Cys500 is coordinated to T1 copper and forms a hydrogen bond with the main chain amide NH group of Leu502, and the presence of Pro444 prevents the formation of a second NH–S hydrogen bond. According to the amino acid sequence (Figure 2), this Pro residue, which is located in a β -strand connecting T1 copper and the TNC, is highly conserved in other MCOs comprised of three domains such as CueO. This Pro residue is not conserved in MCOs that have either six or two domains such as ceruloplasmin or the small laccase of *Streptomyces coelicolor* (SLAC). Therefore, we introduced mutations at Pro444 to study the effect of the NH–S hydrogen bond on the activity of CueO. Analogous mutations have been performed for blue copper proteins, amicyanin (16, 17) and pseudoazurin (18), which have only the blue copper center (T1 copper). These mutations lead to shifts in redox potential from 265 to 380 or 415 mV and from 270 to 409 mV,

		1*	2	3		313	1	1		
CueO	441	ML	PF	IH	NGT	496	YMA	CHLLE	EDTG	MML
Bilirubin Oxidase	396	WT	PI	IH	ILV	453	YMF	CHNLI	EDHD	MMA
CotA	417	GT	PI	HL	HLV	488	YVWH	CHILE	EDYD	MMR
Fet3p	411	GT	PF	HL	HGH	480	WFFH	CHIEW	LLQGL	GL
<i>R. vernicifera</i> Laccase	431	TS	PM	HL	HGF	492	WFLH	CHFER	TTTEG	MAT
Ascorbate Oxidase	443	ET	HP	WL	HGH	503	WAFH	CHIEP	HLHMG	GV
SLAC	229	YY	HT	FM	HGH	284	WMYH	CHVQS	ISMDG	MVG
Ceruloplasmin	973	DL	HT	VH	FGH	1017	WLLH	CHVTD	ITHAG	ET

FIGURE 2: Sequence alignment of MCOs. The numbers 1–3 denote the T1 copper, T2 copper, and T3 copper ligands, respectively. SLAC is the small laccase from *S. coelicolor*.

respectively. The loss of the NH–S hydrogen bond from azurin, in turn, results in a negative shift from 297 to 212 mV (19). Recently, the combined effects of both the axial ligand and hydrogen bond have been studied as factors for tuning the redox potential of azurin (20).

In this study, we investigated the role of hydrogen bonds in the redox potential of T1 copper and laccase activities of CueO by constructing a second NH–S hydrogen bond through mutations at Pro444 and by removing the hydrogen bond between His443, which coordinates to T1 copper, and Asp439 in the outer sphere.

MATERIALS AND METHODS

Preparation of Mutants. The genes for Pro444Gly, Pro444Ala, Pro444Leu, Pro444Ile, Asp439Ala, Leu502Pro, and Asp439Ala/Pro444Ala were prepared using a QuikChange kit (Stratagene). The oligonucleotide primers except for Asp439Ala (15) are listed below, and the underlined codon indicates the mutation: P444G(+), 5'-catgtagctgcatggttccatcatccacg-3'; P444G(-), 5'-cgtggatattggaacccatgcagcatcatg-3'; P444A(+), 5'-catgtagctgcatggttccatcatccacg-3'; P444A(-), 5'-cgtggatattggaacccatgcagcatcatg-3'; P444L(+), 5'-catgtagctgcatgtgttccatcatccacg-3'; P444L(-), 5'-cgtggatattggaacacatgcagcatcatg-3'; P444I(+), 5'-catgtagctgcatatttccatcatccacg-3'; P444I(-), 5'-cgtggatattggaagatgcagcatcatg-3'; L502P(+), 5'-gcgcactgccatccgctggagcatgaa-3'; L502P(-), 5'-ttcatgtctccagcggatggcagtcgcg-3'. Plasmid pUCCueO or pUCCueO $\Delta\alpha 5-7$ was used as a template (11, 12).

E. coli BL21(DE3) was transformed with the mutant plasmids. Cultivation of the transformants and purification of the mutant proteins were conducted as described previously (11, 12). Protein concentrations were determined using the BCA (bicinchoninic acid) Protein Assay Reagent according to the manufacturer's directions (Pierce). Three values were averaged for each mutant and were ascertained to be the same as the values obtained from the absorption intensities at 280 nm: $\epsilon = 73000$ and $70000 \text{ M}^{-1} \text{ cm}^{-1}$ for rCueO and $\Delta\alpha 5-7$ CueO, respectively.

Enzymatic Activities. Activities of the mutants toward oxidation of 2,2'-azinobis(3-ethylbenzothiazoline-6-sulfonic acid) (ABTS), which functions simply as an electron donor, were determined colorimetrically from changes in the absorption of the oxidized product of ABTS at 420 nm ($\epsilon = 36000 \text{ M}^{-1} \text{ cm}^{-1}$) in acetate buffer (0.1 M, pH 5.5) (4, 11). At least three data points were averaged.

Measurements. The total copper content per protein molecule was determined on a Varian SpectraAA-50 atomic absorption spectrometer. Absorption spectra were recorded with a JASCO V-560 spectrometer. Circular dichroism (CD) spectra were recorded on a JASCO J-500C spectropolarimeter. X-Band EPR spectra were measured on a JEOL JES-REIX spectrometer at 77 K. Resonance Raman scattering of the CueO mutants (0.3–3 mM) was excited at 590 nm with an Ar^+ laser (Spectra Physics, 2017)-pumped dye (Rhodamine-6G) laser (Spectra

Table 1: Catalytic Constants,^a Redox Potentials,^b and Copper Contents^c of the Single and Double Mutants of rCueO and $\Delta\alpha 5-7$ CueO at Pro444 and Asp439

	rCueO derivative			$\Delta\alpha 5-7$ CueO derivative		
	Cu content (no. of atoms/protein)	k_{cat} (s ⁻¹)	$E^{\circ'}$ (V vs Ag AgCl)	Cu content (no. of atoms/protein)	k_{cat} (s ⁻¹)	$E^{\circ'}$ (V vs Ag AgCl)
scaffold protein	4.2	0.98 ± 0.021	0.36	3.7	38 ± 0.99	0.37
Pro444Gly	—	—	—	3.1	50 ± 0.54	0.40^d
Pro444Ala	4.1	8.7 ± 0.14	0.43^e	2.8	23 ± 0.14	0.40^d
Pro444Leu	4.3	10 ± 0.44	0.40^e	2.2	17 ± 0.12	0.40^d
Pro444Ile	3.6	5.7 ± 0.10	0.40^e	—	—	—
Asp439Ala	4.2	17 ± 0.66	0.43^e	3.7	147 ± 3.9	0.42^e
double mutant ^f	3.9	40 ± 0.24	0.46^e	3.2	15 ± 0.53	$(0.45)^e$

^a k_{cat} values for ABTS were determined from the change in absorption at 420 nm ($\epsilon = 36000 \text{ M}^{-1} \text{ cm}^{-1}$) in acetate buffer (pH 5.5). ^bDetermined by electrochemistry. ^cDetermined by atomic absorption spectroscopy. ^dFormal potential (vs Ag|AgCl) determined by direct electrochemistry using an Au disk electrode and thioglycolate as a promoter. Potentials were calibrated to the values for a carbon cryogel electrode. ^eEstimated from the shift in potential at which the cathodic current to reduce O_2 began to flow. ^fAsp439Ala/Pro444Ala.

Physics, 376) and detected with a CCD (Princeton Instruments) attached to a triple polychromator (JASCO, NRS-1800) at room temperature. The laser power was 50 mW at the sample point. Thirty scans (accumulation time, 1 s each) were averaged. One to three data sets were collected and averaged. Toluene and acetone were used as references. The error in peak position was $< 1 \text{ cm}^{-1}$ except for that of the double mutant, Asp439Ala/Pro444Ala ($< 2 \text{ cm}^{-1}$), in which spectrum contributions from the oxidizing agent, sodium hexachloroirridate(IV) were subtracted. A BAS CV50-W potentiostat was used for cyclic voltammetry and a BAS rotator RDE-1 for rotating disk voltammetry under O_2 . As the working electrode, either carbon cryogel (15) or an Au electrode modified with thioglycolate was used. A Pt wire and an Ag|AgCl|saturated KCl electrode were used as counter and reference electrodes, respectively. All measurements were taken in McIlvaine buffer (0.1 M, pH 5), adjusted to an ionic strength of 0.5 with K_2SO_4 under 1 atm of O_2 or Ar using a water-jacketed cell at 25 °C or in phosphate buffer (0.1 M, pH 6) under Ar. Formal potentials determined using the carbon cryogel electrode shifted 0.22 V toward the positive direction relative to those determined using the modified Au electrode, and accordingly, the latter potentials were corrected to the values determined using the carbon cryogel electrode.

RESULTS

Formation of an NH-S Hydrogen Bond in Pro444 Mutants. The Pro444 mutants of rCueO with Ala, Leu, and Ile substitutions were found to contain four copper atoms per protein molecule within an experimental error of 10% as ascertained by atomic absorption spectroscopy (Table 1). Absorption, CD, and EPR spectra of these mutants are shown in Figure 3A–C (black, blue, green, and red for rCueO, Pro444Ala, Pro444Leu, and Pro444Ile, respectively). All mutants exhibited an absorption band derived from T1 copper at $\sim 610 \text{ nm}$, while the absorption maximum wavelength was shifted 2–3 nm toward shorter wavelengths from that of rCueO (9, 10). The intensity of this band of the Ala and Ile mutants was weaker ($\epsilon = 4900 \text{ M}^{-1} \text{ cm}^{-1}$) than that of rCueO ($\epsilon = 6500 \text{ M}^{-1} \text{ cm}^{-1}$). Further, the spectrum of each of the mutants has another absorption band at $\sim 330 \text{ nm}$ derived from T3 coppers bridged with a hydroxide ion ($\epsilon = 5900\text{--}6500 \text{ M}^{-1} \text{ cm}^{-1}$), which is, in turn, slightly more intense than that of rCueO ($\epsilon = 5400 \text{ M}^{-1} \text{ cm}^{-1}$). The CD spectra exhibit more complex spectral features from the absorption spectra because the absorption band at $\sim 610 \text{ nm}$ is comprised of the charge transfer bands, $\text{S}^-(\text{Cys})_{\sigma} \rightarrow \text{Cu}^{2+}$ and

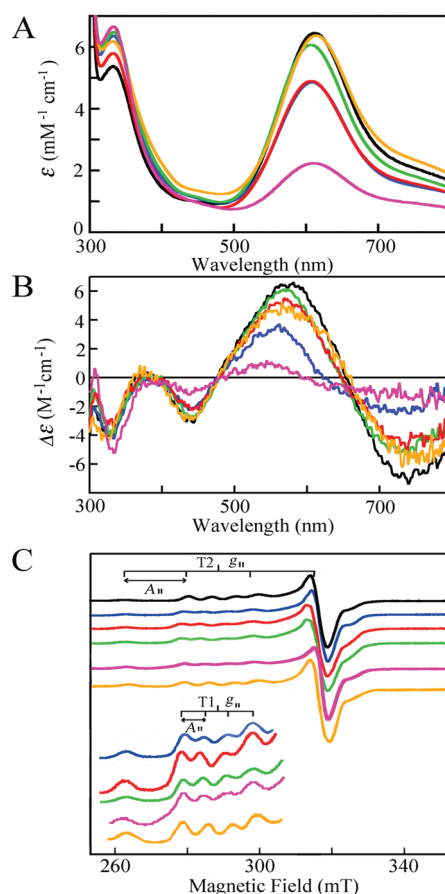


FIGURE 3: Absorption (A), CD (B), and EPR (C) spectra of rCueO (black) and mutants, Pro444Ala (blue), Pro444Ile (red), Pro444Leu (green), Asp439Ala (ocher), and Asp439Ala/Pro444Ala (magenta). Absorption and CD spectra of $\sim 100 \mu\text{M}$ proteins in 0.1 M phosphate buffer (pH 6) were recorded at room temperature using a 1 cm path length quartz cell. The units of the ordinate are based on the protein molecule. EPR spectra were recorded at 77 K with a frequency of 9.2 GHz, a microwave power of 4 mW, a modulation amplitude of 1 mT, a T1 copper of 100 kHz, a filter of 0.3 s, a sweep time of 4 or 8 min, and an amplitude of 200–400.

$\text{S}^-(\text{Cys})_{\pi} \rightarrow \text{Cu}^{2+}$, and is accompanied by the strong d–d band in the 700–900 nm range as well as the charge transfer band at 330 nm (9, 10). Pro444Ile has slightly weakened CD bands relative to those of rCueO in the 500–800 nm range, although four copper atoms per protein molecule were determined within experimental error. On the other hand, the Pro444Ala mutant was found to have modified CD spectral features relative to those of rCueO in the

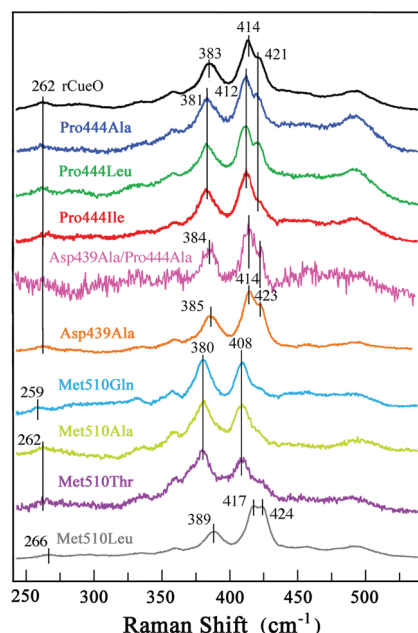


FIGURE 4: Resonance Raman spectra of rCueO (black), Pro444Ala (blue), Pro444Ile (red), Pro444Leu (green), Asp439Ala (ocher), Asp439Ala/Pro444Ala (magenta), Met510Gln (pale blue), Met510Ala (pale green), Met510Thr (purple), and Met510Leu (gray). Measurement conditions are given in Materials and Methods.

500–800 nm range. EPR spectra of the Pro444 mutants have two signals originating from T1 copper and T2 copper with small and normal magnitudes of hyperfine splitting, respectively ($A_{\parallel} = 6.7\text{--}6.9 \times 10^{-3}$ and $18\text{--}19 \times 10^{-3} \text{ cm}^{-1}$, respectively). EPR signals caused by T3 coppers were not detected in any of the mutants because of the strong antiferromagnetic interaction. This indicates that the mutations at Pro444 do not affect the magnetic properties of the remote TNC.

Resonance Raman spectra of rCueO and the Pro444 mutants are shown in Figure 4 (black, blue, green, and red for rCueO and the Ala-, Leu-, and Ile-containing mutants, respectively). Many Raman bands were observed in the range of $250\text{--}450 \text{ cm}^{-1}$ because of the coupling of the Cu(II)–S(Cys) stretching and Cys deformation modes (21). The strongest Raman band was observed at 414 cm^{-1} for rCueO but was found to be shifted to 412 cm^{-1} in the Ala, Leu, and Ile mutants. This indicates that the Cu(II)–S(Cys) bond is slightly weakened as a result of the mutations that form the second NH–S hydrogen bond.

rCueO differs from the other MCOs by having little or no laccase activity (no activity for 2,6-dimethoxyphenol and very low activity for ABTS and *p*-phenylenediamine) (11). This is also the case for the Pro444 mutants. However, ABTS-oxidizing activities were easily determined for the Pro444 mutants with an absorption spectrometer (Table 1) and were found to have increased by 6–10-fold (9, 10). Rotating disk voltammetry measurements of the Pro444 mutants under O_2 indicated that cathodic currents begin to flow at $\sim 500 \text{ mV}$ (vs Ag|AgCl). This is 40–70 mV more positive than the analogous measurement taken for rCueO (Figure 5 and Table 1). The cathodic current densities did not become saturated when the rate of rotation of the working electrode was increased. This indicates that the electron that entered the protein molecule through T1 copper was effectively transferred to O_2 under diffusion limiting conditions (15, 22, 23). The cathodic current densities produced by the Pro444 mutants of $2\text{--}4 \text{ mA/cm}^2$ were 25–50% of those of

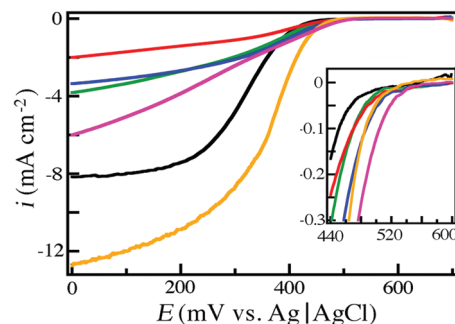


FIGURE 5: Background-subtracted cyclic voltammograms of rCueO (black), Pro444Ala (blue), Pro444Ile (red), Pro444Leu (green), Asp439Ala (ocher), and Asp439Ala/Pro444Ala (magenta) with a carbon cryogel electrode under O_2 . Measurement conditions: scan rate of 20 mV/s , rotation rate of 2000 rpm , 0.1 M McIlvaine buffer, pH 5, ionic strength of $0.5 (\text{K}_2\text{SO}_4)$, Pt counter electrode, Ag|AgCl reference electrode, and temperature of 25°C .

rCueO whose cathodic current density is 8 mA/cm^2 . However, these values are still much higher than those obtained from other MCOs such as bilirubin oxidase and fungal laccases (24, 25), although improvements have recently been attained for these MCOs (22).

We generated analogous mutations of Pro444 for $\Delta\alpha 5\text{--}7$ CueO with Gly, Ala, and Leu (the same amino acid numbering scheme is used for amino acid residues in rCueO and $\Delta\alpha 5\text{--}7$ CueO to avoid confusion). The copper content of the Pro444Gly, Pro444Ala, and Pro444Leu mutants was found to be 3.1, 2.8, and 2.2 coppers per protein molecule, respectively (Table 1). The copper content could not be improved in spite of modifications of the culture conditions and reactions with cupric or cuprous ions after purification of the mutants. The absorption spectra of these mutants included weakened 610 and 330 nm bands (Figure S1 of the Supporting Information). However, the absorption intensity at 610 nm of the Pro444Gly mutant increased from 3900 to $5500 \text{ M}^{-1} \text{ cm}^{-1}$ upon reaction with a small amount of sodium hexachloroirridate(IV), a strong oxidizing agent (spectrum not shown). This indicates that the T1 copper center in Pro444Gly had been fully occupied by copper ions, but not in the Pro444Ala and Pro444Leu mutants. This suggests that the mutants are mixtures of holoproteins, apoproteins, and proteins with partially occupied copper centers. CD and EPR spectra exhibited features analogous to those of rCueO except for decreases in intensity. In contrast to the Pro444 mutations of rCueO, the Pro444 mutations of $\Delta\alpha 5\text{--}7$ CueO have the strongest band at 414 cm^{-1} and have the same Raman shift as rCueO and $\Delta\alpha 5\text{--}7$ CueO (Figure S2 of the Supporting Information). The only apparent change was observed in the 1 cm^{-1} shift in the shoulder of Pro444Gly at 422 cm^{-1} . In spite of less copper incorporation, the Gly mutant has greater ABTS oxidizing activity ($k_{\text{cat}} = 50 \text{ s}^{-1}$) than $\Delta\alpha 5\text{--}7$ CueO ($k_{\text{cat}} = 38 \text{ s}^{-1}$). Although the Ala and Leu mutants have slightly lower activities than $\Delta\alpha 5\text{--}7$ CueO, the k_{cat} values (23 and 17 s^{-1} , respectively) were much higher than that of rCueO (0.98 s^{-1}). The redox potentials of these mutants are $\sim 30 \text{ mV}$ more positive than that of $\Delta\alpha 5\text{--}7$ CueO. This was directly determined by cyclic voltammetry using an Au electrode modified with thioglycolate because electrochemical responses of the $\Delta\alpha 5\text{--}7$ CueO-based mutants were stronger than those of the rCueO-based mutants (Figure S3A of the Supporting Information and Table 1).

Breakdown of a Hydrogen Bond in Asp439 Mutants. The Asp439Ala mutant of rCueO contained four copper atoms per molecule within an experimental error of 10% (Table 1).

Absorption intensities of Asp439Ala at 610 and 330 nm were almost the same as those of rCueO (indicated by the ocher color in Figure 3A). In addition, no change was observed in the CD and EPR spectra (ocher in Figure 3B,C). The strongest Raman band was observed at 414 cm^{-1} . This is the same Raman shift as that of rCueO (ocher in Figure 4). However, the bands at 383 and 421 cm^{-1} shifted to 385 and 423 cm^{-1} , respectively, indicating that the Cu(II)–S(Cys) bond is slightly strengthened by the mutation to break down the hydrogen bond between Asp439 and His443 that is coordinated to T1 copper. On the other hand, no appreciable shift was observed in the resonance Raman bond due to the Cu(II)–N bond at 262 cm^{-1} . Electrochemistry of Asp439Ala under O_2 indicated that the redox potential shifted by ca. 70 mV in the positive direction (Figure 5B). The catalytic constant, k_{cat} , for the oxidation of ABTS by Asp439Ala was 17 s^{-1} . This is 17 times higher than that of rCueO (Table 1).

In contrast to the Pro444 mutants of $\Delta\alpha 5-7$ CueO, four copper atoms were contained in the Asp439Ala mutant of $\Delta\alpha 5-7$ CueO and gave absorption, CD, and EPR spectra that were similar to those of rCueO (Figure S1 of the Supporting Information and Table 1). The resonance Raman spectrum of Asp439Ala $\Delta\alpha 5-7$ CueO has bands at 421, 415, and 385 cm^{-1} . The latter two bands have increases of 1–2 cm^{-1} from the corresponding bands of $\Delta\alpha 5-7$ CueO and the Pro444 mutants (Figure S2 of the Supporting Information). The ABTS oxidizing activity of this mutant ($k_{\text{cat}} = 147\text{ s}^{-1}$) is ~4-fold higher than that of $\Delta\alpha 5-7$ CueO, with an enhancement of the enzymatic activity of 150-fold relative to that of rCueO (Table 1). Electrochemical measurements of Asp439Ala $\Delta\alpha 5-7$ CueO indicated a positive shift of ~50 mV in the redox potential from that of $\Delta\alpha 5-7$ CueO (Figure S3B of the Supporting Information).

Asp439 and Pro444 Double Mutants. Expecting to attain great increases in activity, we prepared the Asp439Ala/Pro444Ala double mutants of rCueO and $\Delta\alpha 5-7$ CueO. The copper content of the double mutant of rCueO was 3.9 coppers per protein molecule (Table 1), but the absorption intensity at 610 nm ($\epsilon = 2400\text{ M}^{-1}\text{ cm}^{-1}$) was ~36% of that of rCueO (Figure 3A, magenta). However, the reaction of Asp439Ala/Pro444Ala rCueO with a slight excess of sodium hexachloroiridate(IV) resulted in a prominent increase in the absorption intensity that was as strong as that of rCueO (Figure S4A of the Supporting Information). This suggests that the redox potential of T1 copper undergoes a positive potential shift to favor the cuprous state. On the other hand, the absorption intensity at 330 nm is similar to that of rCueO. The CD spectrum (Figure 3B, magenta) exhibits features analogous to that of Asp439Ala with prominently decreased intensities in the bands originating from T1 copper, while they were increased by the reaction with hexachloroiridate(IV) (Figure S4B of the Supporting Information). On the other hand, the EPR signal intensity of T1 copper of the Asp439Ala/Pro444Ala rCueO mutant is also slightly weak relative to that of rCueO (Figure 3C, magenta) but increases after the reaction with hexachloroiridate(IV) (not shown). Electrochemical data of Asp439Ala/Pro444Ala rCueO indicate that the redox potential of T1 copper is ~460 mV, the greatest positive shift of 100 mV from that of rCueO (Figure 5). The resonance Raman spectrum has bands at 384, 414, and 423 cm^{-1} (Figure 4, magenta), and these are shifted by at most 1 cm^{-1} from the corresponding bands of rCueO. The k_{cat} value of the double mutant is increased by ~40-fold (40 s^{-1}) from that of rCueO (0.98 s^{-1}), indicating that the cumulative effect is an activity

increase of ~10-fold caused by the mutation at Pro444 and ~17-fold caused by the mutation at Asp439 (Table 1).

For the double mutant of $\Delta\alpha 5-7$ CueO, the averaged copper content is 3.2 coppers per protein molecule. The absorption intensity at 608 nm is $3000\text{ M}^{-1}\text{ cm}^{-1}$ (Figure S1A of the Supporting Information, magenta) and increases to $5500\text{ M}^{-1}\text{ cm}^{-1}$ after the reaction with a small amount of hexachloroiridate(IV) (not shown). This indicates that the T1 copper center is almost fully occupied. Therefore, it appears that approximately one-third of the T2 copper and T3 copper centers are vacant in a given sample of this double mutant. A fraction of the TNC appears to be fully occupied because the double mutant exhibits ABTS oxidizing activity ($k_{\text{cat}} = 15\text{ s}^{-1}$), with all of the same expected CD bands and T1 copper and T2 copper EPR signals as rCueO, although their intensities are generally weaker (Figure S1B,C of the Supporting Information, magenta). The electrochemical response of the double mutant was found to be not as high as that of rCueO or $\Delta\alpha 5-7$ CueO, but there was a positive shift in the redox potential by ~80 mV from that of $\Delta\alpha 5-7$ CueO (Figure S3B of the Supporting Information, magenta).

DISCUSSION

The three rCueO mutants with Ala, Leu, and Ile substitutions at Pro444 each contain four copper ions and have absorption and CD spectra similar to those of rCueO, although absorption intensities at 610 nm are slightly decreased and a CD spectral feature of the Ala mutant is modified at wavelengths above 500 nm. Autoreduction of T1 copper or spin delocalization between the coordinating S atom and T1 copper has been frequently observed in certain MCOs and their mutants with high redox potentials (26–28). However, the decreased absorption of the 610 nm band observed for the Pro444Ala and -Ile mutants is more likely to be the result of the second hydrogen bond formed with the S atom coordinated to T1 copper (Figure 3). The pronounced modifications in the CD spectrum of Pro444Ala were reproducible in the three preparations, and accordingly, the formation of the second hydrogen bond led to modifications of the spectral properties related to the Cu(II)–S(Cys) bond. The peculiar CD bands in the visible region have been assigned to the charge transfer bands originating from the $\text{S}^-(\text{Cys}) \rightarrow \text{Cu}^{2+}$ transition, but the S atom itself is not an asymmetric center. Therefore, the so-called vicinal effect due to the asymmetric α -carbon of the Cys residue would be the main contributor in providing the circular dichroism effect for the relevant transition bands, although it is not known why the effect of the mutation at Pro444 is most profound for the Ala substitution. The EPR signals due to T1 copper and T2 copper in the Pro444 mutants are the same as those of rCueO, ensuring that the magnetic properties of both T1 copper and T2 copper are unchanged by the mutations that encourage the formation of the second NH–S hydrogen bond. These small changes in the spectral properties of the Pro444 mutants of rCueO are in harmony with results of the mutation at the Pro80 residue in pseudoazurin (18) in contrast to the Phe114Pro mutant of azurin (19).

In the resonance Raman spectra, the effect of the formation of the second hydrogen bond at the thiolate sulfur coordinating T1 copper in rCueO was observed as a shift in the band at 414 cm^{-1} to one at 412 cm^{-1} (Figure 4). The introduction of the second NH–S hydrogen bond led to a decrease in the negative charge on the thiolate sulfur, resulting in weakening of the Cu(II)–S(Cys) bond. This also accounts for the positive shift in the redox

potential. The weakening of the Cu(II)–S(Cys) bond and shifts in the resonance Raman bands are also reflected in the resonance Raman spectra of Met510Gln, -Thr, and -Ala mutants of rCueO (see Figure 4). An oxygen atom in the side chain of the substituted amino acid residues or an H₂O molecule that may occupy the extra space provided by the Ala mutation and possibly also by the Thr mutation binds more strongly to T1 copper than the thioether of Met. This imposes a rhombic distortion on the T1 copper site (13, 29) and leads to weakening of the Cu(II)–S(Cys) bond and produces a shift in the resonance Raman band from 414 to 408 cm^{−1}. In contrast, the substitution of Met with Leu to produce the tricoordinated T1 copper that is similar to the coordination geometry of fungal laccases produces opposite shifts in the resonance Raman bands due to a stronger Cu(II)–S(Cys) bond and also produces a shift in the redox potential in the positive direction. The bands at 383, 414, and 421 cm^{−1} of rCueO shift to 389, 417, and 424 cm^{−1}, respectively. Thus, resonance Raman spectroscopy is useful for directly demonstrating the slight changes in the strength of the Cu(II)–S(Cys) bond. However, the effect of weakening the Cu(II)–S(Cys) bond derived by the formation of the second NH–S bond might have been offset in the Δα5–7 CueO mutants presumably because of a structural change at the T1 copper center, which might have been induced by deletion of the capped helical region. The slight modifications to the absorption and CD spectra (Figure 3A,B) support this possibility. Crystal structures of rCueO and Δα5–7 CueO indicate that the scaffold protein structure and the structure in the vicinity of the T1 copper center do not change after the deletion of the capped helical segment (Figure 1) (11). However, the effect of additional modifications on the scaffold protein has not been studied in detail. All spectroscopic data for T1 copper are for the cupric form, and no data for the cuprous form, in which the Cu(I)–S(Cys) bond would be expected to have been strengthened by the mutations at Pro444, are available. Although the Cu(II)–N stretch at 262 cm^{−1} is poorly resonance enhanced in these resonance Raman spectra, disrupting the hydrogen bond between Asp439 and His443 does not seem to have an impact on this vibrational mode (Figure 4). Nevertheless, an indirect effect of mutations in the outer sphere of the T1 copper center was observed in the resonance Raman bands of Asp439Ala Δα5–7 CueO as 1–2 cm^{−1} shifts to higher wavenumbers (Figure S2 of the Supporting Information).

The redox potential of T1 copper in the Pro444 mutants shifted in the positive direction by 40–70 mV (Figure 5 and Table 1). These results are consistent with the results of forming or disrupting an NH–S hydrogen bond in blue copper proteins, including amicyanin (17), pseudoazurin (18), and azurin (19). The effect of a hydrogen bond on the tuning of the redox potential of the copper center in blue copper proteins was found not to be as significant as proposed on the basis of quantum mechanical calculations (30), and the effect was even smaller for CueO. Therefore, it appears that the introduction of an NH–S hydrogen bond in MCO is not as significant as it is in the blue copper proteins. This correlates with the accessibility of solvent to the T1 copper center (18). This observation provides an indication that the redox potential of T1 copper in MCO is determined by a variety of factors such as the polarity at the copper site, the set of ligands and their steric characteristics, and the reorganization energy of the protein molecule accompanied by the redox change in addition to the hydrogen bond. In line with this, an increase in the activity of CueO by a factor of 5 has also been realized because of the 40 mV positive shift in the redox potential of T1

copper caused by the Leu substitution at the axially coordinating Met510, a mutation with the goal of mimicking the T1 copper center of fungal laccases (13). The NH–S hydrogen bond is apparently one of the dominating factors used to tune the redox potential of MCOs and the oxidizing activities of various substrates in addition to providing a stabilizing effect for the protein molecule (vide infra). The S(Cys) atom coordinating to the T1 copper center in ceruloplasmin is doubly hydrogen-bonded because of the absence of a Pro residue (Figure 2) (14). This protein exhibits a redox potential higher than that of T1 copper in CueO. Similarly, mutation of Pro399 in bilirubin oxidase produces a protein with a nearly fully reduced T1 copper center strongly resistant to oxidation (unpublished results).

Positive shifts in the redox potential of T1 copper in the Pro444 mutants have been considered to be due to the induction of an electric dipole on the NH–S hydrogen bond, and electrostatic repulsion toward the cupric ion (31). Alternatively, formation of the second NH–S bond might have led to a delocalization of the thiolate sulfur negative charge and stabilization of the copper ion (16, 17).

As a result of the mutations that introduce the second NH–S bond, the enzyme activity levels of CueO increased by ~6–10-fold as indicated in Table 1. This might favor electron transfer between ABTS and T1 copper because the positive shift in the redox potential of T1 copper would outweigh the effect of the long-range electron transfer from T1 copper to TNC through the His-Cys-His triad. In line with this, flash photolysis data obtained for CueO suggest that the initial electron transfer from 5-deazariboflavin semiquinone to T1 copper is one of the steps governing the overall enzymatic activity (2).

The Pro444Gly mutation of Δα5–7 CueO enhances the activity (1.3-fold). This does not occur for the corresponding Ala and Leu mutants (Table 1). The averaged copper content of these mutants was found to be approximately two to three per protein molecule. Therefore, these mutants represent a mixture of holoprotein, apoprotein, and proteins with partial incorporation of copper. It was found that apoprotein is not present in the Pro444Gly mutant of Δα5–7 CueO because the T1 copper center was fully occupied (Figure S1 of the Supporting Information). The enzymatic activities listed in Table 1 have been undoubtedly derived from holoproteins, but the normalized enzymatic activity due to holoproteins could not be evaluated because their exact content could not be determined. In the Ala and Leu mutants, it has been more difficult to evaluate the holoprotein content. Therefore, we did not correct enzymatic activities by normalization. It seems that the enhancements in the enzymatic activities shown by the Pro444 mutants of Δα5–7 CueO are still considerably low even taking into consideration the presence of apoprotein and protein with partial incorporation of copper. The T1 copper center in Δα5–7 CueO is no longer deeply buried inside the protein molecule as a result of the deletion of the methionine-rich helical region covering the active site (11). This might have caused an increase in the reorganization energy accompanied by the change in the redox state of T1 copper. On the other hand, the prominent reduction in the copper content of the Leu502Pro mutant, in which the original NH–S hydrogen bond would have been lost (data not shown), indicates that at least one NH–S hydrogen bond is required to stabilize the T1 copper site. Therefore, it appears that the NH–S hydrogen bond plays a dual role in stabilizing the structure around the T1 copper center and tuning the redox potential.

The effect of breaking the hydrogen bond between His443 (which coordinates to T1 copper) and Asp439 contrasts with the effect of forming the NH–S hydrogen bond. The loss of the hydrogen bond from the coordinated His residue produces a positive shift of 50–70 mV in the redox potential and increases the enzymatic activity of rCueO and $\Delta\alpha 5-7$ CueO by ~20- and ~4-fold, respectively. The Asp439 mutations of $\Delta\alpha 5-7$ CueO did not reduce the number of incorporated copper ions or affect the absorption, CD, and EPR spectra. These results are in contrast with the Pro444 mutations of $\Delta\alpha 5-7$ CueO that caused the copper content of the protein molecule to partially decrease and the T1 copper center to become slightly unstable. The loss of the hydrogen bond simply produced a shift in the redox potential of T1 copper without affecting the stability of the T1 copper site or the protein molecule. This is presumably because the hydrogen bond is not directly formed with the coordinating N^{δ1} atom, in contrast to the mutations of Pro444 (vide infra). The ability to donate the imidazole N^{δ1} atom to T1 copper might have been weakened by the disruption of the NH–O hydrogen bond. This would lead to a shutdown of the resonance interaction between N^{δ1} and N^{ε2} in the imidazole ring, although this is not reflected in the resonance Raman band for the Cu(II)–N bond at 262 cm^{−1}, presumably because of the difficulty in observing smaller frequency shifts in the low-frequency modes. Analogous to the mutation of CueO, Asp409 in Fet3p has been changed to Ala to study substrate specificity. This mutant has a 120 mV positive shift in the redox potential of T1 copper, while the increase in ferroxidase activity has been reported to be only 20% (32).

With the expectation of observing a synergistic effect on ABTS oxidizing activity, the Asp439 and Pro444 double mutants were prepared for rCueO and $\Delta\alpha 5-7$ CueO. In the rCueO Asp439Ala/Pro444Ala double mutant, more than two-thirds of the T1 coppers are in the cuprous state (Figure 3), and the expected cumulative effect of forming and deleting hydrogen bonds has been ascertained by the greatest positive shift of 100 mV in the redox potential (Figure 5). The largest increase in activity of 40-fold relative to that of rCueO (Table 1) was realized in spite of an unfavorable shift in the redox potential of T1 copper for the intramolecular electron transfer from T1 copper to TNC. If we could modify the redox potential of TNC to a more positive potential near the potential for dioxygen reduction (0.82 V at pH 7), further increases in activity would be expected. On the other hand, the copper content of the double mutant of $\Delta\alpha 5-7$ CueO remains at approximately three per protein molecule as observed for the single mutants of Pro444 (Figure S1 of the Supporting Information), although the T1 copper center is fully occupied as ascertained by the reaction with hexachloroirridate(IV). The increase in activity is 15-fold greater relative to that of rCueO and 0.4-fold relative to that of $\Delta\alpha 5-7$ CueO. This suggests that there is a limit to which a protein molecule can be modified.

CONCLUSIONS

The enzymatic activities of CueO increase with mutations at Pro444 that encourage the formation of a second hydrogen bond between the backbone NH group of the mutated amino acid and the thiolate sulfur coordinating the T1 copper center. This increase appears to be due to altered Cu–S(Cys) bond strength and redox potential. Disruption of the hydrogen bond between His443 (which is coordinated to T1 copper) and Asp439 also produces mild modifications that lead to increases in activity. A synergistic effect on the redox potential of T1 copper and enzyme

activity was realized by preparation of a double mutant with mutations at Asp439 and Pro444. Modifications to form or break a hydrogen bond are widely applicable to every MCO and related metalloproteins. The ability to tune the redox properties of the T1 copper center of CueO provides an opportunity to offset the higher overpotentials required by CueO compared to bilirubin oxidase and fungal laccases for electrochemistry and biofuel cell applications.

ACKNOWLEDGMENT

We thank Prof. Kenji Kano, Asst. Prof. Seiya Tsujimura, Dr. Maiko Tsutsumi, and Mr. Masafumi Asahi of Kyoto University (Kyoto, Japan) for performing the electrochemical measurements.

SUPPORTING INFORMATION AVAILABLE

Absorption, CD, and EPR spectra of $\Delta\alpha 5-7$ CueO mutants, resonance Raman spectra of $\Delta\alpha 5-7$ CueO mutants, electrochemical data of $\Delta\alpha 5-7$ CueO mutants, and absorption and CD spectra of Asp439Ala/Pro444Ala rCueO reacted with hexachloroirridate(IV). This material is available free of charge via the Internet at <http://pubs.acs.org>.

REFERENCES

1. Outten, F. W., Huffman, D. L., Hale, J. A., and O'Halloran, T. V. (2001) The independent *cue* and *cus* systems confer copper tolerance during aerobic and anaerobic growth in *Escherichia coli*. *J. Biol. Chem.* 276, 30670–30677.
2. Roberts, S. A., Weichsel, A., Grass, G., Thakali, K., Hazzard, J. T., Tollin, G., Rensing, C., and Montfort, W. R. (2002) Crystal structure and electron transfer kinetics of CueO, a multicopper oxidase required for copper homeostasis in *Escherichia coli*. *Proc. Natl. Acad. Sci. U.S.A.* 99, 2766–2771.
3. Roberts, S. A., Wildner, G. F., Grass, G., Weichsel, A., Ambrus, A., Rensing, C., and Montfort, W. R. (2003) A labile regulatory copper ion lies near the T1 copper site in the multicopper oxidase CueO. *J. Biol. Chem.* 278, 31958–31963.
4. Grass, G., Thakali, K., Klebba, P. E., Thieme, D., Müller, A., Wildner, G. F., and Rensing, C. (2004) Linkage between catecholate siderophores and multicopper oxidase CueO in *Escherichia coli*. *J. Bacteriol.* 186, 5826–5833.
5. Singh, S. K., Grass, G., Rensing, C., and Montfort, W. R. (2004) Cuprous oxidase activity of CueO from *Escherichia coli*. *J. Bacteriol.* 186, 7815–7817.
6. Ueki, Y., Inoue, M., Kurose, S., Kataoka, K., and Sakurai, T. (2006) Mutations at Asp112 adjacent to the trinuclear Cu center in CueO as the proton donor in the four-electron reduction of dioxygen. *FEBS Lett.* 580, 4069–4072.
7. Kataoka, K., Sugiyama, R., Hirota, S., Inoue, M., Urata, K., Minagawa, Y., Seo, D., and Sakurai, T. (2009) Four-electron reduction of dioxygen by a multicopper oxidase, CueO, and roles of Asp¹¹² and Glu⁵⁰⁶ located adjacent to the trinuclear copper center. *J. Biol. Chem.* 284, 14405–14413.
8. Iwaki, M., Kataoka, K., Kajino, T., Sugiyama, R., Morishita, H., and Sakurai, T. (2010) ATR-FTIR study of the protonation states of the Glu residue in the multicopper oxidases, CueO and bilirubin oxidase. *FEBS Lett.* 584, 4027–4031.
9. Sakurai, T., and Kataoka, K. (2007) Basic and applied features of multicopper oxidases, CueO, bilirubin oxidase, and laccase. *Chem. Rec.* 7, 220–229.
10. Sakurai, T., and Kataoka, K. (2007) Structure and function of type I copper in multicopper oxidases. *Cell. Mol. Life Sci.* 64, 2642–2656.
11. Kataoka, K., Komori, H., Ueki, Y., Konno, Y., Kamitaka, Y., Kurose, S., Tsujimura, S., Higuchi, Y., Kano, K., Seo, D., and Sakurai, T. (2007) Structure and function of the engineered multicopper oxidase CueO from *Escherichia coli*: Deletion of the methionine-rich helical region covering the substrate-binding site. *J. Mol. Biol.* 373, 141–152.
12. Kurose, S., Kataoka, K., Otsuka, K., Tsujino, Y., and Sakurai, T. (2007) Promotion of laccase activities of *Escherichia coli* cuprous oxidase, CueO by deleting the segment covering the substrate binding site. *Chem. Lett.* 36, 232–233.

13. Kurose, S., Kataoka, K., Shinohara, N., Miura, Y., Tsutsumi, M., Tsujimura, S., Kano, K., and Sakurai, T. (2009) Modification of spectroscopic properties and catalytic activity of *Escherichia coli* CueO by mutations of methionine 510, the axial ligand to the type I Cu. *Bull. Chem. Soc. Jpn.* 82, 504–508.
14. Bento, I., Peixoto, C., Zaitzev, V. N., and Lindley, P. F. (2007) Ceruloplasmin revised: Structural and functional roles of various metal cation-binding sites. *Acta Crystallogr. D* 63, 240–248.
15. Miura, Y., Tsujimura, S., Kurose, S., Kataoka, K., Sakurai, T., and Kano, K. (2009) Direct electrochemistry of CueO and its mutants at residues to and from near type I Cu for oxygen-reducing biocathode. *Fuel Cells* 9, 70–78.
16. Machczynski, M. C., Gray, H. B., and Richards, J. H. (2002) An outer-sphere hydrogen-bond network constrains copper coordination in blue proteins. *J. Inorg. Biochem.* 88, 375–380.
17. Carrell, C. J., Sun, D., Jiang, S., Davidson, V. L., and Mathews, F. S. (2004) Structural studies of two mutants of amicyanin from *Paracoccus denitrificans* that stabilize the reduced state of the copper. *Biochemistry* 43, 9372–9380.
18. Nishiyama, M., Suzuki, J., Ohnuki, T., Chan, H. C., Horinouchi, S., Turley, S., Adman, E. T., and Beppu, T. (1992) Site-directed mutagenesis of pseudoazurin from *Alcaligenes faecalis* S-6; Pro80Ala mutant exhibits marked increase in reduction potential. *Protein Eng.* 5, 177–184.
19. Yanagisawa, S., Banfield, M. J., and Dennison, C. (2006) The role of hydrogen bonding at the active site of a cupredoxin: The Phe114Pro azurin variant. *Biochemistry* 45, 8812–8822.
20. Marshall, N. M., Garner, D. K., Wilson, T. D., Gao, Y. G., Robinson, H., Nilges, M. J., and Lu, Y. (2009) Rationally tuning the reduction potential of a single cupredoxin beyond the natural range. *Nature* 462, 113–116.
21. Han, J., Adman, E. T., Beppu, T., Codd, R., Freeman, H. C., Huq, L. L., Loehr, T. M., and Sanders-Loehr, J. (1991) Resonance Raman spectra of plastocyanin and pseudoazurin: Evidence for conserved cysteine ligand conformations in cupredoxins (blue copper proteins). *Biochemistry* 30, 10904–10913.
22. Tsujimura, S., Kamitaka, Y., and Kano, K. (2007) Diffusion-controlled oxygen reduction on multi-copper oxidase-adsorbed on carbon aerogel electrodes without mediator. *Fuel Cells* 7, 463–469.
23. Tsujimura, S., Miura, Y., and Kano, K. (2008) CueO-immobilized porous carbon electrode exhibiting improved performance of electrochemical reduction of dioxygen to water. *Electrochim. Acta* 53, 5716–5720.
24. Shleev, S., Tkac, J., Christenson, A., Ruzgas, T., Yaropolov, A. I., Whittaker, J. W., and Gorton, L. (2005) Direct electron transfer between copper-containing proteins and electrodes. *Biosens. Bioelectron.* 20, 2517–2554.
25. Cracknell, J. A., Vincent, K. A., and Armstrong, F. A. (2008) Enzymes as working or inspirational electrocatalysts for fuel cells and electrolysis. *Chem. Rev.* 108, 2439–2461.
26. Shimizu, A., Sasaki, T., Kwon, J.-H., Odaka, A., Satoh, T., Sakurai, N., Sakurai, T., Yamaguchi, S., and Samejima, T. (1999) Site-directed mutagenesis of a possible type I copper ligand of bilirubin oxidase; a Met467Gln mutant shows stellacyanin-like properties. *J. Biochem.* 125, 662–668.
27. Shimizu, A., Kwon, J.-H., Sasaki, T., Satoh, T., Sakurai, N., Sakurai, T., Yamaguchi, S., and Samejima, T. (1999) *Myrothecium verrucaria* bilirubin oxidase and its mutants for potential copper ligands. *Biochemistry* 38, 3034–3042.
28. Sakurai, T. (2006) The alkaline transition of blue copper proteins, *Cucumis sativus* plastocyanin and *Pseudomonas aeruginosa* azurin. *FEBS Lett.* 580, 1729–1732.
29. Tsai, L. C., Bonander, N., Harata, K., Karlsson, G., Vänngård, T., Langer, V., and Sjölin, L. (1996) Mutant Met121Ala of *Pseudomonas aeruginosa* azurin and its azide derivative: Crystal structures and spectral properties. *Acta Crystallogr. D* 52, 950–958.
30. Li, H., Webb, S. P., Ivanic, J., and Jensen, J. H. (2004) Determinants of the relative reduction potential of type-I copper sites in proteins. *J. Am. Chem. Soc.* 126, 8010–8019.
31. Olsson, M. H. M., Hong, G., and Warshel, A. (2003) Frozen density functional free energy simulations of redox proteins: Computational studies of the reduction potential of plastocyanin and rusticyanin. *J. Am. Chem. Soc.* 125, 5025–5039.
32. Stoj, C. S., Augustine, A. J., Zeigler, L., Solomon, E. I., and Kosman, D. J. (2006) Structural basis of the ferrous iron specificity of the yeast ferroxidase, Fet3p. *Biochemistry* 45, 12741–12749.
33. DeLano, W. L. (2002) The PyMOL Molecular Graphics Systems, DeLano Scientific, San Carlos, CA.